Multiscale Fusion of Wavelet-Domain Information and Clustering Analysis for Digital Halftoning

He Zifen[1] Zhang Yinhui[1]* Zhan Zhaolin[2] Wang Sen[1]

[1] *Faculty of Mechanical and Electrical Engineering, Kunming University of Science and Technology, Kunming, Yunnan 650500, China*

[2] *Faculty of Materials Science and Engineering, Kunming University of Science and Technology, Kunming, Yunnan 650093, China*

Abstract A novel approach to improve the halftoning image quality by a mixture distortion criterion is the combination of a edge weighted least squares depending on the fusion multiscale information and the region weighted least squares depending on the improved K-means clustering method. The multiscale characterization of the original image using the discrete wavelet transform is obtained. The boundary information of the target image is fused by the wavelet coefficients of the correlation between wavelet transform layers, to increase the pixel resolution scale. The inter-scale fusion method to gain fusion coefficient of the fine-scale is applied, which takes into account the detail of the image and approximate information, where the fusion coefficient is referred to as the weighting operator, and to establish the boundary energy function. The improved K-means clustering method is used to segment an image several regions and the new energy function is constructed using the weighted least squares method, which the reciprocal of the variance of the segmented regions are referred to as the weighting operator to establish the region energy function. In the halftone process, each clustering uses the weighted least-squares method through energy minimization via direct binary search algorithm, to gain halftoning image. Simulation results on typical test images further confirm the performance of the new approach.

Key words imaging processing; halftoning; multiscale information fusion; improved K-means clustering; weighted least-squares; direct binary search

OCIS codes 100.2810; 110.2960; 150.1135

多尺度融合小波域信息和聚类分析的数字半色调

何自芬[1] 张印辉[1] 詹肇麟[2] 王 森[1]

([1]昆明理工大学机电工程学院，云南 昆明 650500；[2]昆明理工大学材料科学与工程学院，云南 昆明 650093)

摘要 提出采用小波域多尺度信息融合的方法建立数字半色调尺度相关的误差测度函数。利用尺度间小波系数的自相关性融合层间的小波细节系数，采用加权最小平方法建立边缘误差测度函数。应用改进的 K-means 聚类法将原图像分割为几个区域，利用各区域方差倒数做为权重，建立区域误差测度函数。应用改进直接二值搜索方法最小化初始图像和半色调图像的误差，得到最优的数字半色调图像。模拟结果表明了提出算法的有效性。

关键词 图像处理；半色调；多尺度信息融合；改进 K 均值聚类；加权最小平方；直接二值搜索

中图分类号 TP391 **文献标识码** A **doi**：10.3788/CJL201441.s109003

1 Introdution

Many image rendering technologies only have binary output such as the laser engraving gravure, laser beam printer, laser plate-maker and digital printer. Binary halftoning would try to compute a pattern of binary dots to achieve the illusion of a multi-bit image. Halftone image contains a series of dots in a specific pattern that simulates the look of a continuous tone image. The

收稿日期：2013-10-23；**收到修改稿日期**：2013-11-14

基金项目：国家自然科学基金(61302173,60962007)

作者简介：何自芬(1976—)女，博士，讲师，主要从事图像处理、机器视觉和微光刻技术方面的研究。E-mail：zyhhzf1998@163.com

* **通信联系人**。E-mail：zhangyinhui@kmust.edu.cn

multiscale fusion of wavelet-domain information and clustering analysis (MFWICA) halftone algorithm presented in this paper is a new halftone algorithm that seeks to improve halftone image quality by enhancing the gray image smoothness and sharpness between regions and edges.

According to computational style, the halftoning algorithms can be classified into three categories[1]: Neighborhood based methods, such as error diffusion[2], point based methods, such as screening[3] and look-up-table[4] and iterative optimization methods[5], which uses a human visual system model to minimize the perceived error.

The goal of model-based halftoning techniques is to exploit explicit models of the display device and the human visual system (HVS) to maximize the quality of the displayed images[6]. The iterative techniques include one-dimensional Viterbi algorithm to obtain the globally optimal solution[7], blocking with branch and bound minimization[8], and diffusion-reaction model[9]. Least-squares method-based (LSMB) halftoning approach attempts to produce an optimal halftone reproduction[10].

In this paper, we extend this technique for the proposed algorithm. The boundary information of the target image is fused by the wavelet coefficients of the correlation between wavelet transform layers, which to increase the pixel resolution scale. We apply the inter-scale fusion method to gain fusion coefficient of the fine-scale, which takes into account the details of the image and approximate informations and establish the boundary energy function. The complexity of the visual tasks when viewing halftones prompts us to consider the image to be comprised of features more complex than simple edges. That is, we consider the image to be comprised of regions, some that can be characterized by local variations and some that can not. We seek to identify these regions that contain texture and to render to achieve different visual effects in the different parts of the image in response to edge and region contents.

2 Multiscale fusion wavelet-domain information

2.1 Two-discrete wavelet transform

The Haar wavelet transform may be considered to simply pair up the input values, storing the difference and passing the sum[11]. This process is repeated recursively, pairing up the sums to provide the next scale, finally resulting in 2^{n-1} differences and one final sum.

Let ϕ^{LL} denote scale function, $\{\varphi^{LH},\varphi^{HL},\varphi^{HH}\}$ denote the wavelet function. The scale function and wavelet function form $L^2(R^2)$ space orthogonal basis. The image $f(x,y)$, decomposed in the space domain with the size of $N\times N$, can be expressed as

$$f(x.\,y)=\sum_{k,j=0}^{N_j-1}u_{J,k,i}\phi^{LL}_{J,k,i}(x,y)+\sum_{b\in B}\sum_{j=1}^{J}\sum_{k,i=0}^{N_{j-1}}w^{b}_{j,k,i}\varphi^{b}_{j,k,i}(x,y),\tag{1}$$

where $\phi^{LL}_{J,k,i}(x,y)=2^{-j/2}\phi(x/2^j-k,y/2^j-i)$ and $\varphi^{b}_{j,k,i}(x,y)=2^{-j/2}\varphi^{b}(x/2^j-k,y/2^j-i)$, $b\in B$, $B=\{LH,HL,HH\}$ is the wavelet coefficients in three sub-band directions, $N_j=N/2$. The scale coefficients $u_{J,k,i}$ and wavelet coefficients $w^{b}_{j,k,i}$ in j scale subband B direction are given as

$$u_{J,k,i}=\iint f(x,y)\phi^{LL}_{J,k,i}(x,y)\,\mathrm{d}x\mathrm{d}y,$$
$$w^{b}_{j,ki}=\iint f(x,y)\varphi^{b}_{j,k,i}(x,y)\,\mathrm{d}x\mathrm{d}y.\tag{2}$$

Given the scale and node of the wavelet coefficient $w^{b}_{j,k,i}$, its father node is $w^{b}_{j+1,[k/2],[i/2]}$. $[\cdot]$ denotes round numbers, and its four sub-nodes are $w^{b}_{j-1,2k,2i}$, $w^{b}_{j-1,2k,2i+1}$, $w^{b}_{j-1,2k+1,2i}$, and $w^{b}_{j-1,2k+1,2i+1}$.

The transform from spatial domain to wavelet domain can provide a compact representation of the original image. The multiscale information is shown in Fig. 1.

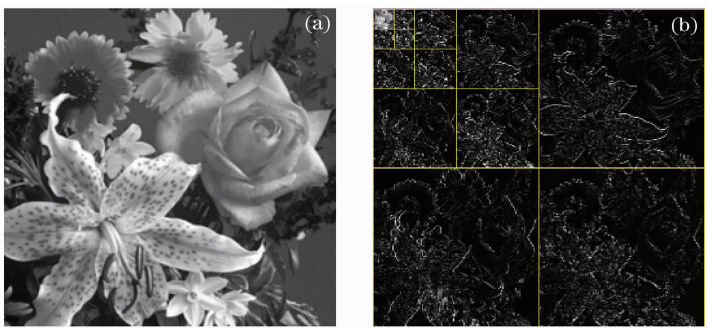

Fig. 1 Original image (a) and the four levels discrete wavelet transform (b)

We can see that most of the image energy compacted onto a few wavelet coefficient, with large magnitudes while most of the wavelet coefficients are very small. This compact property allows us to capture the key characteristics of an image from a few large wavelet coefficients.

2.2 Wavelet coefficients fusion

Since most of the wavelet coefficients have small values, only a few wavelet coefficients have large values. Upon the assumption that the wavelet coefficients are mutually independent, they are normalized. The boundary information of the target image is fused by the wavelet coefficients of the correlation between wavelet transform layers to increase the pixel resolution scale. We apply the inter-scale fusion method to gain fusion coefficient of the fine-scale, which takes into account the details of the image and approximate information. The fusion information of inter-scale wavelet coefficients is shown in Fig. 2.

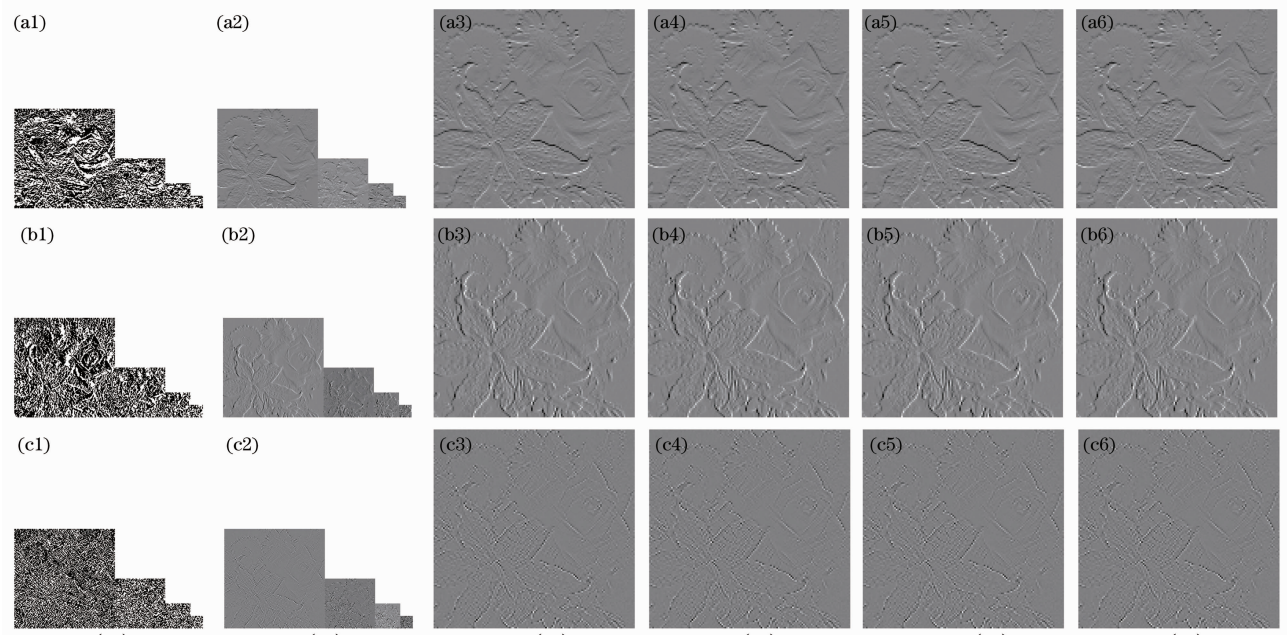

Fig. 2 Fusion information of inter-scale wavelet coefficients for (a) HL, (b) LH and (c) HH sub-bands. (a1),(b1),(c1) 4-scales wavelet coefficients, (a2),(b2),(c2) 4- scales wavelet coefficients normalized, (a3),(b3),(c3) scale 0 and 1 fusion, (a4),(b4),(c4)scale 0,1 and 2 fusion, (a5),(b5),(c5) scale 0 ,1,2 and 3 fusion (a6),(b6),(c6) scale 0, 1, 2,3 and 4 fusion

3 Image segmentation

Fast global K-means clustering algorithm is an improved global K-means clustering algorithm by Aristidis Likas[12].

We use the improve K-means clustering that needs to determine the number of cluster classes and distance measurements to determine the degree of similarity between pixels and classes. The gray image is partitioned into two, three and four regions via the improved K-means image segmentation method. Each label shows a different class. Seen from Fig. 3, there are two , three and four regions generated by the clustering,

Table 1 Pixels statistics for each cluster

	Cluster	$1/\sigma$
1	$K=$Ⅰ	0.0039
2	$K=$Ⅰ	0.0014
	K=Ⅱ	0.0009
3	$K=$Ⅰ	0.0027
	$K=$Ⅱ	0.0017
	$K=$Ⅲ	0.0025
4	$K=$Ⅰ	0.0065
	$K=$Ⅱ	0.0060
	$K=$Ⅲ	0.0033
	$K=$Ⅳ	0.0020

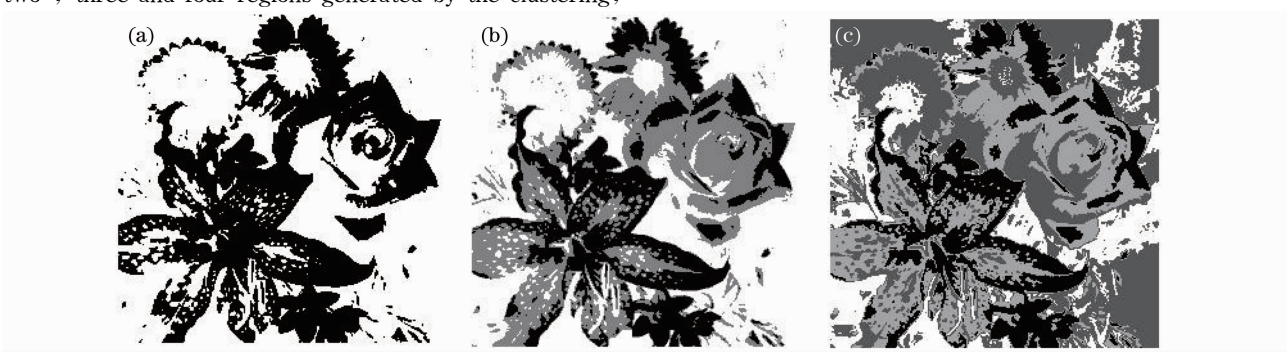

Fig. 3 Image labels by cluster index K. (a) $K=2$; (b) $K=3$; (c) $K=4$

which the original image gray value display area of each block and the outside the gray area are shown as 0. The statistics of the mean and variance of the gray-scale pixel of each clustering are calculated. They are shown in Table 1.

4 Energy function minimization

We will use the term contrast sensitivity here, since we have used this terminology throughout Mannos and Sakrison[13] proposed a model of the human contrast sensitivity function, and found the following filter frequency response to be good for predicting the subjective quality of the coded images.

$$H_r(f_r) = 2.6 \times (0.0192 + 0.114 f_r) \times \exp[-(0.114 f_r)^{1.1}], \quad (3)$$

f_r in Eq. (3) is the spatial frequency of the visual stimuli given in cycles/degree. The function has a peak value 1 approximately at $f_r = 8.0$ cycles/degree, and is meaningless for frequencies above 60 cycles/degree. LSMB halftoning attempts to produce an optimal halftoned reproduction[10]. In this article, we will use the following notation. Suppose we are given a gray-scale image $[x_{i,j}]$, where $x_{i,j}$ denotes the pixel located at the i-th column and the j-th row of a grid. The gray level of each pixel varies from 0 equal to white to 1 equal to black. Assuming that the image has been sampled, there is one pixel per dot to be generated. Thus the gray-scale image array $[x_{i,j}]$ and the binary image array $[b_{i,j}]$ have the same dimensions. We are also given a printer model with the sliding-window form and an eye model of the form with a memory-less nonlinearity $n(\cdot)$ followed by an FIR filter with impulse response $[h_{i,j}]$. In the LSMB approach we seek the halftone image that minimizes the squared error.

$$E = \sum_{i,j} (z_{i,j} - w_{i,j})^2, \quad (4)$$

where $z_{i,j} = n(x_{i,j}) * h'_{i,j}$, $w_{i,j} = n(p_{i,j}) * h_{i,j}$, $p_{i,j} = P(W_{i,j})$, $W_{i,j}$ is composed of $b_{i,j}$, its neighbors and $*$ indicates convolution. Note that we have allowed different impulse responses $h_{i,j}$, $h'_{i,j}$ for the eye filters corresponding to the halftone and continuous-tone images respectively. The boundary conditions assume that no ink is placed outside the image borders.

Weighted least squares model-based regression is useful for estimating the values of model parameters when the response values have different degrees of variability over the combinations of the predictor values[14]. Optimal results that minimize the uncertainty in the parameter estimators are obtained when the weights used to estimate the values of the unknown parameters are inversely proportional to the variances at each combination of predictor variable values $\sigma i \propto 1/\sigma_i^2$.

In the proposed approach, we seek the halftone image that minimizes the weighted squared error

$$E_{i,j} = \left\{ \sum_{l=1}^{4} (\mathrm{LH}, \mathrm{HL}, \mathrm{HH}) + \sum_{k=1}^{4} \right\} \sum_{i,j} (z_{i,j} - w_{i,j})^2. \quad (5)$$

The k ($k = 1,2,3,4$) are weighting operators and $*$ indicates convolution. Note that we have allowed different impulse responses for the eye filters corresponding to the halftone and continuous-tone images.

The goal of DBS is to determine the binary halftone image $g[m, n]$ such that the difference between the perceived versions of the original gray-scale image and the rendered halftone is minimized[15]. As a measure of the difference, the total squared error is equal. We model the low pass characteristic of the eye with a luminance spatial frequency response function.

We compute this error efficiently by computing first the autocorrelation function of the filter, $c_{\bar{p}\bar{p}}$ and the correlation between the error and the filter, $c_{\bar{p}\bar{p}}$. The error is a function of those two. Each time we try a change, then we can evaluate the consequences of this change on the error by using only four values of these matrix. If the change we tried effectively reduces the error, it is accepted, and this time we need to change as many values of $c_{\bar{p}\bar{p}}$ as there are values in $c_{\bar{p}\bar{p}}$. This is acceptable though, because especially in the last passes over the image, we try much more changes than the number we accept.

5 Experimental results and discussions

The input $x(i,j)$ is a grayscale image quantized to 256 discrete gray levels normalized to 1. It is assumed that x has dimensions $N \times N$, where N is a power of 2. In this paper, we use the 'flowers' image of sizes 256×256 to demonstrate the experimental results. All halftones are generated and printed at a resolution of 300 inch^{-1} and 24 inches viewing distance. We use the MFWICA algorithm to obtain the halftone images. In the experiment, we compare two algorithms: the LSMB, and the proposed algorithm.

Fig. 4 LSMB halftoning

The results show that this method achieves the better quality halftones that combines smooth gray tone reproduction and good edge and detail reproduction in the same image. This is illustrated qualitatively in Fig. 5. They show the combination of desirable smooth and sharp visual effects by applying the technique to a "flowers" image. Fig. 4 shows the LSMB halftone image. For comparison, Fig. 5(a) ~ (d) show the results of applying a "smooth" constraint, λ_1, λ_2, λ_3 and λ_4, at every pixel in the image and the results of applying a "sharp" constraint of wavelet fusion parameters inter-scale at every pixel in the image. On testing with many images, we confirm it when comparing the quality measurements of halftone images with MSE and PSNR. The test results are shown in Table 2. It is clear from both Table 2 that the proposed algorithm achieves consistently lower values of MSE than the LSMB algorithm, and with the increase in cluster partition, the value of MSE is also decreases. We can be seen from Table 2 that the proposed algorithm achieves consistently higher values of PSNR than the LSMB algorithm, and with the increase in cluster partition, the value of PSNR are also increase.

The parameter that needs to be selected is the termination condition in the experiment, which is selected as 10^{-2} during the running of the program. The result is illustrated in Fig. 6. Note that all of the convergence errors dropped down to the termination condition within 15 iterations. The proposed algorithm is terminated with 8 iterations. Therefore the convergence of the proposed algorithm is relatively rapid.

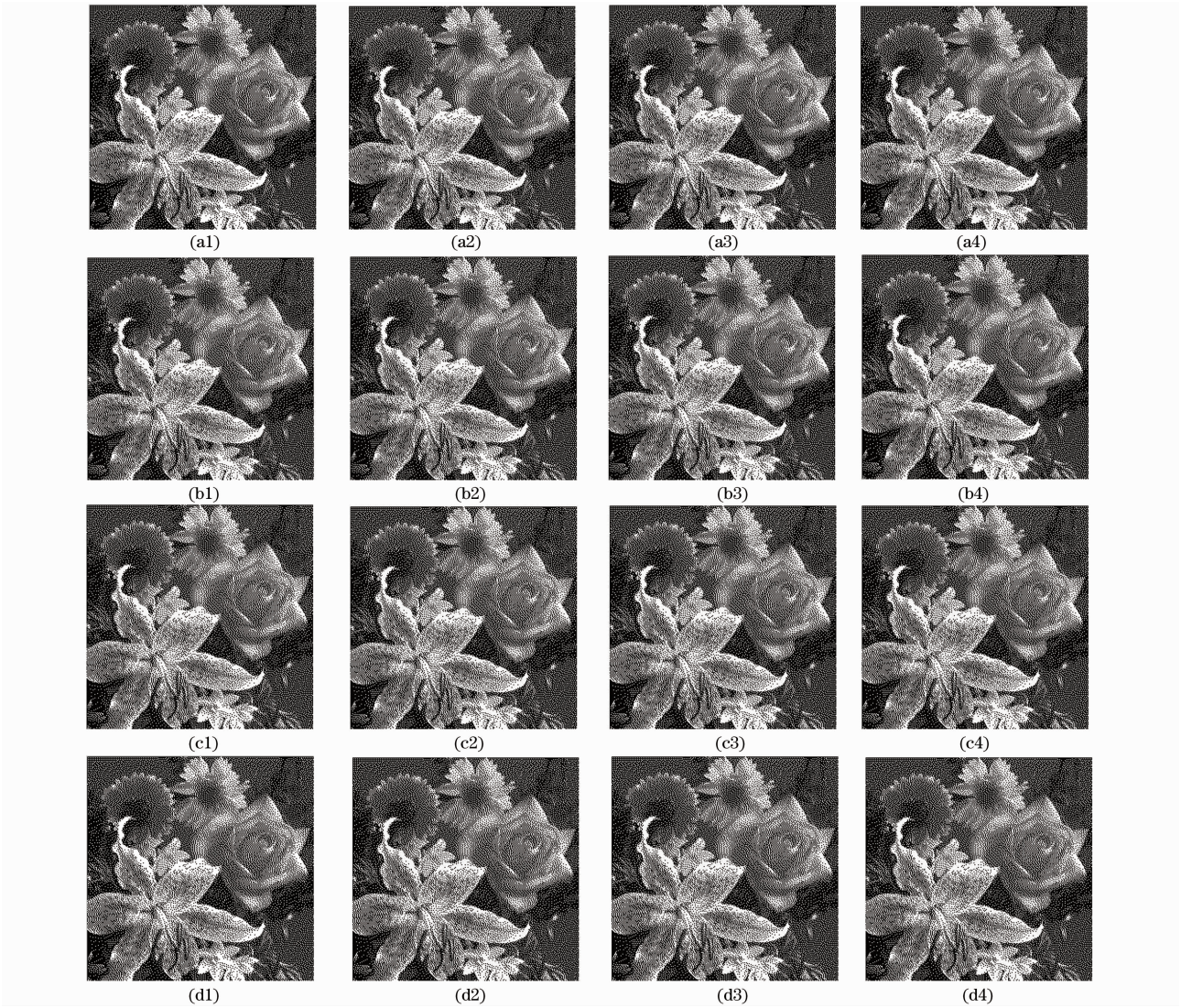

Fig. 5 Proposed algorithm in (a) $K = 1$ with weighted operator λ_1, (b) $K = 2$ with weighted operators λ_1 and λ_2, (c) $K = 3$ with weighted operators λ_1, λ_2 and λ_3, (d) $K = 4$ with weighted operators λ_1, λ_2, λ_3 and λ_4. (a1),(b1),(c1),(d1) halftoning scales 0 and 1 fusion, (a2),(b2),(c2),(d2) halftoning scales 0, 1 and 2 fusion, (a3),(b3),(c3),(d3) halftoning scales 0,1, 2 and 3 fusion, (a4),(b4),(c4),(d4) halftoning scales 0,1,2,3 and 4 fusion

Table 2　Quality measurement of halftones with different algorithms in terms of MSE and PSNR

Algorithm	Cluster	Weighted operator	Wavelet coefficients fusion	MSE /10^{-3}	PSNR /dB
LSMB				0.1261	27.12
Proposed	1	λ_1	Scale 0 and 1	0.1174	27.69
			Scale 0, 1 and 2	0.1156	27.79
			Scale 0, 1, 2 and 3	0.1143	28.86
			Scale 0, 1, 2, 3 and 4	0.1055	29.92
	2	λ_1 and λ_2	Scale 0 and 1	0.0974	30.69
			Scale 0, 1 and 2	0.0897	31.96
			Scale 0, 1, 2 and 3	0.0732	32.41
			Scale 0, 1, 2, 3 and 4	0.0621	33.74
	3	λ_1, λ_2 and λ_3	Scale 0 and 1	0.0537	35.24
			Scale 0, 1 and 2	0.0501	36.18
			Scale 0, 1, 2 and 3	0.0485	36.99
			Scale 0, 1, 2, 3 and 4	0.0402	37.05
	4	λ_1, λ_2, λ_3 and λ_4	Scale 0 and 1	0.0275	37.81
			Scale 0, 1 and 2	0.0203	38.94
			Scale 0, 1, 2 and 3	0.0121	39.06
			Scale 0, 1, 2, 3 and 4	0.0071	39.84

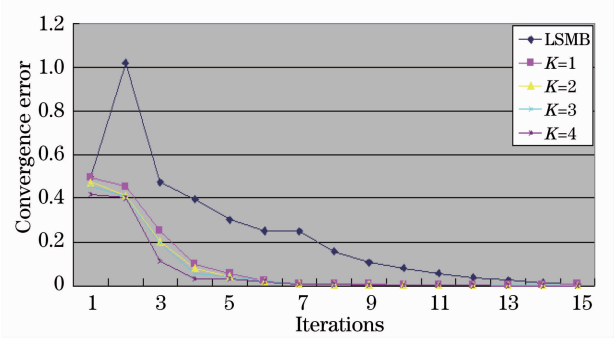

Fig. 6　Comparison of the number of iterations for the test image

6　Conclusion

In this work, we have proposed a multiscale information fusion method of wavelet-domain for halftoning. Our method can fusion the boundary information presented in the approximation coefficients and regional information presented in the improved K-means clustering method. Therefore the energy term is generated, which consists of both boundary and regional terms. We have identified the "flowers" image and tested the MSE and PSNR of the proposed method. Quantitative evaluation of algorithm shows that our method is superior to the LSMB method in the iterations speed. Our future work will be emphasized on improved optimize method of the multiscale energy functions based algorithm.

References

1 J P Allebach. Selected Papers on Digital Halftoning [M]. Bellingham: SPIE Press, 1999.

2 R W Floyd, L Steinberg. An adaptive algorithm for spatial grey-scale[J]. Proc SID, 1976, 17(2): 75 - 77.

3 B E Bayer. An optimum method for two-level rendition of continuous-tone pictures[C]. IEEE Int Conf Commun, 1973, 1: 26.11 - 26.15.

4 P Li, J Allebach. Look-up-table based halftoning algorithm[J]. IEEE Trans Image Processing, 2000, 9(9): 1593 - 1603.

5 M Analoui, J Allebach. Model-based halftoning using direct binary search[C]. SPIE, 1992, 1666: 96 - 108.

6 Sang Ho Kim, Jan P Allebach. Impact of HVS models on model-based halftoning[J]. IEEE Trans Image Process, 2002, 11(3): 258 - 269.

7 DL Neuhoff, T N Pappas, N Seshadri. One-dimensional least - squares model-based halftoning[C]. Proceedings of ICASSP-93, 1992, 3: 189 - 192.

8 A Zakhor, S Lin, F Eskafi. A new class of B/W halftoning algorithms[J]. IEEE Trans Image Processing, 1993, 2(4): 499 - 509.

9 A Sherstinsky, R W Picard. M-lattice: a novel non-linear dynamical system and its application to halftoning[C]. Proc IEEE Conf Acoustics, 1994, 2: 565 - 568.

10 Thrasyvoulos N Pappas, David L Neuhoff. Least-quares model-based halftoning[J]. IEEE Trans Image Processing, 1999, 8(8): 1102 - 1116.

11 A Haar. Zur Theorie der orthogonalen funktionensysteme[J]. Math Ann, 1910, 69(3): 331 - 371.

12 A Likas, N Vlassis, J J Verbeekb. The global k-means clustering algorithm[J]. Pattern Recognition, 2003, 36(2): 451 - 461.

13 J L Mannos , D J Sakrison. The effects of a visual fidelity criterion of the encoding of images[J]. IEEE Trans Information Theory, 1974, 20(4): 525 - 536.

14 W S Cleveland, S J Devlin. Locally weighted regression: an approach to regression analysis by local fitting[J]. J Am Stat Assoc, 1988, 83(403): 596 - 610.

15 F A Baqai, C C Taylor, J P Allebach. Halftoning via direct binary search using a hard circular dot overlap model[C]. Proc IS&T/OSA Optics & Imaging in the Information Age, 1996. 383 - 391.

栏目编辑：何卓铭